https://doi.org/10.48047/AFJBS.6.12.2024.6531-6559

African Journal of Biological Sciences

Journal homepage: http://www.afjbs.com

Research Paper Open Access

MANAGEMENT OF TINEA VERSICOLOR BY USING NANOPARTICLE OPTIMIZED TOPICAL DRUG LULICONAZOLE

[1]Kritika Singh, *[2]Anupriya Adhikari, [3]Shivanand M Patil

[1]Research Scholar, Shree Dev Bhoomi Institute of Education Science and Technology (SDBIT), Dehradun, INDIA.

[2]Associate Professor, Shree Dev Bhoomi Institute of Education Science and Technology (SDBIT), Dehradun, INDIA.

[3]Professor, Shree Dev Bhoomi Institute of Education Science and Technology (SDBIT), Dehradun, INDIA.

Corresponding Author: adhikari02anupriya@gmail.com

Volume 6, Issue 12, June 2024

Received: 01 May 2024

Accepted: 25 May 2024

Published: 15 June 2024

doi: 10.48047/AFJBS.6.12.2024.6531-6559

Abstract:
A paper titled "Formulation and Evaluation of Polymeric Nanoparticles for Optimized Luliconazole Delivery in Tinea Versicolor Management" paves the way for additional research and applications in the field of dermatological treatments. Nanoparticle formulations could be improved by using advanced nanotechnology techniques, such as nanoscale targeting strategies and stimuli-responsive drug release mechanisms. This is one of the prospective directions that could be pursued. It is possible that this will improve the specificity and efficacy of the administration of luliconazole, hence reducing the number of off-target effects and increasing the number of therapeutic results. There is also the possibility that future research will concentrate on doing in vivo studies in order to evaluate the efficacy, pharmacokinetics, and safety of the improved nanoparticle formulations in animal models of tinea versicolor. These kinds of investigations would offer extremely helpful insights into the translational potential of the formulations that have been produced for practical usage in clinical settings. Furthermore, there is a requirement for comparative studies to evaluate the performance of the nanoparticle-based delivery system in comparison to the performance of existing treatment modalities. These treatment modalities include conventional topical formulations and oral antifungal drug formulations. In the context of the management of tinea versicolor, this comparative analysis would shed light on the relative benefits and drawbacks of drug delivery based on nanoparticles. In addition, given the growing interest in personalized medicine, it is possible that future research could investigate the possibility of tailoring nanoparticle formulations to individual patient characteristics, such as the type of skin, the severity of the disease, and genetic predispositions, in order to maximize the effectiveness of treatment and minimize the negative effects. This research paper in its entirety, lays the framework for further innovation and advancement in the development of nanoparticle-based drug delivery systems for enhanced management of tinea versicolor and other dermatological disorders.
Keywords: Tinea versicolor, Disease, Polymer, Nanoparticles, Luliconazoles

Introduction

Tinea versicolor, a superficial fungal infection caused by the Malassezia genus, is characterized by the appearance of hypopigmented or hyperpigmented patches on the skin, typically on the trunk, neck, and upper arms [1]. While not considered medically serious, it can cause considerable distress due to its cosmetic effects. The challenges in treating tinea versicolor lie in its tendency for recurrence and the emergence of antifungal resistance. Current treatment modalities mainly include topical antifungal agents like ketoconazole, selenium sulfide, or oral medications such as fluconazole [2]. However, these treatments often necessitate prolonged use, leading to issues of patient compliance and potential side effects such as skin irritation or systemic toxicity. Addressing these challenges, researchers are exploring innovative approaches, including the utilization of polymeric nanoparticles in treatment strategies. Polymeric nanoparticles offer several advantages, including improved drug solubility, enhanced stability, and controlled release kinetics [3]. By encapsulating antifungal agents within biocompatible polymer matrices, nanoparticles can facilitate targeted delivery to the affected skin areas, thereby enhancing drug penetration and bioavailability while minimizing systemic exposure and adverse effects. Moreover, the sustained release provided by polymeric nanoparticles could potentially prolong the therapeutic effect, addressing the issue of recurrence in tinea versicolor treatment [4]. This approach holds promise for optimizing treatment efficacy and patient outcomes while minimizing the burden of prolonged therapy and associated side effects. Further research into the formulation, characterization, and clinical application of polymeric nanoparticles in tinea versicolor treatment is warranted to realize their full potential in clinical practice.

Material & Method

This study aimed to use chitosan as a polymeric carrier for the drug Luliconazole, and improve its stability, solubility, and bioavailability using commonly used excipients such as mannitol and lactose in nanoparticle formulation. The organic solvents dimethyl sulfoxide and ethanol were used, along with cholesterol and PEG 2000. The equipment used in the study included a probe sonicator and a magnetic stirrer.

Preparation of Polymeric Nanoparticles by Solvent Evaporation Method:

Measure the required amounts of polyethylene glycol, soya lecithin, cholesterol, and dimethyl sulfoxide. Mix polyethylene glycol, soya lecithin, and cholesterol in ethanol. This mixture will serve as the organic phase. Dissolve Luliconazole (the drug) in DMSO and then dilute it in distilled water. This will be the aqueous phase. Slowly add the organic phase (containing the dissolved lipids) drop by drop into the aqueous phase (containing the drug). Use a high-speed homogenizer or sonicator to create an emulsion. Place the emulsion in a rotary evaporator. Evaporate the organic solvent (DMSO and ethanol) under reduced pressure, leaving behind the drug-loaded polymeric nanoparticles. Centrifuge the solution to separate the nanoparticles. Wash the nanoparticles with distilled water to remove any residual solvent. Centrifuge the solution to separate the nanoparticles. Wash the nanoparticles with distilled water to remove any residual solvent. Several medications are available for the treatment of tinea versicolor, ranging from topical antifungal agents to oral medications. Commonly prescribed topical antifungals include ketoconazole, which is available in various formulations such as creams, shampoos, and foams, and works by inhibiting the synthesis of ergosterol, a crucial component of fungal cell membranes. Selenium sulfide is another topical option that exerts its antifungal effect by inhibiting the growth of Malassezia yeasts [12]. Other topical agents like ciclopirox, terbinafine, and clotrimazole may also be used, although they are less frequently prescribed for tinea versicolor. For more extensive or refractory cases, oral antifungal medications such as fluconazole, itraconazole, or ketoconazole may be recommended. These systemic agents act by disrupting fungal cell membrane integrity or interfering with ergosterol synthesis [13]. However, their use may be limited by potential side effects and drug interactions, necessitating careful consideration and monitoring by healthcare providers. Additionally, maintenance therapy with antifungal shampoos or creams may be prescribed to prevent recurrence. While these medications are generally effective in treating tinea versicolor, challenges such as patient compliance, the risk of adverse effects, and the emergence of antifungal resistance highlight the need for ongoing research to optimize treatment strategies and improve outcomes for affected individuals.

Evaluation of formulated batches:

Percentage yield and entrapment efficiency of formulation batches

Yield percentage and entrapment efficiency are crucial evaluation criteria for formulation quantities. The percentage yield reflects the efficiency of the formulation process as a whole by comparing the actual quantity of the desired product obtained to its theoretical yield. A process that produces a high percentage yield is more efficient and cost-effective.

Yield Percentage = *(Weight of PEG-Nanoparticles/Total expected weight of extract and excipients) × 100*

Entrapment efficacy, on the other hand, quantifies the formulation's capacity to effectively encapsulate and retain the target substance. It is especially applicable in the development of drug delivery systems, where the objective is to obtain maximum drug entrapment within the carrier system. A high entrapment efficiency guarantees that a greater proportion of the active ingredient is effectively conveyed to the target site, thereby enhancing therapeutic efficacy and minimizing waste.

Entrapment efficiency (%) = *(Calculated drug content/Theoretical drug content) × 100*

In-vitro release of formulation

The in-vitro release of all batches of nano suspension was carried out using the dialysis bag method. A clean dialysis bag was soaked in distilled water, filled with a specified amount of polymeric nanoparticle suspension, and sealed with thread. This sealed bag was then placed into a dissolution apparatus containing 900 ml of PBS at pH 7.4. The temperature was maintained at 37°C ± 0.5°C, and the apparatus was set to 100 rpm. Samples were collected at various intervals, ensuring sink conditions were maintained by replacing the withdrawn samples with fresh PBS. The drug content in the samples was analyzed by diluting them and measuring absorbance using a UV-visible spectrophotometer at 296 nm. The formulation demonstrating the highest encapsulation efficiency (EE%) and drug release was chosen for further studies

FTIR of Formulation batches & excipients.

The FTIR (Fourier Transform Infrared Spectroscopy) results are crucial for analyzing and characterizing formulation batches. FTIR spectroscopy is a robust analytical method that offers

essential insights into the chemical composition and structural properties of the samples. By measuring the absorption and interaction of infrared radiation with the molecules in the formulation, FTIR spectra offer insights into the functional groups, molecular bonds, and overall chemical fingerprint of the samples.

The FTIR results allows to identify and confirm the presence of specific functional groups and chemical bonds in the formulation. This information is crucial for assessing the chemical integrity and stability of the product. Additionally, FTIR analysis can detect any potential chemical interactions or transformations that may occur during the formulation process, including degradation, impurities, or changes in molecular structure. The FTIR of optimized batches of PEGylated nanoparticles with their interpretation is shown below in result section

Evaluation of formulation:

Percentage yield and entrapment efficiency of formulation batches

The entrapment efficiency of nanoparticles was determined using the centrifugal-ultrafiltration method. The supernatant obtained after centrifuging the nanoparticles was analyzed for the amount of unentrapped drug using spectrophotometric absorption at 296 nm [79]. A 2 ml aliquot of the drug-loaded complexes was placed in the upper chamber of a centrifuge tube equipped with a centrifugal-ultrafiltration device. The concentration of the samples was then calculated based on standard curves. All experiments were conducted at 25°C. The entrapment efficiency and loading capacity were calculated using the following equations:

Drug loading (%) = (Amount of drug loaded in complex / Total weight of complex) × 100

Entrapment efficiency (%) = [(Weight of drug added – Free drug in supernatants) / Weight of drug added] × 100

Table 1: Percentage yield and encapsulation efficiency of the batches

Formulation Batches	Percentage Yield (%)	Entrapment efficiency (%)
F1	56.84	55.24

F2	60.23	65.14
F3	77.12	78.86
F4	54.45	60.41
F5	54.78	62.54
F6	81.4	86.7
F7	66.3	72.5
F8	79.98	80.19
F9	77.6	82.9
F10	83.2	84.01

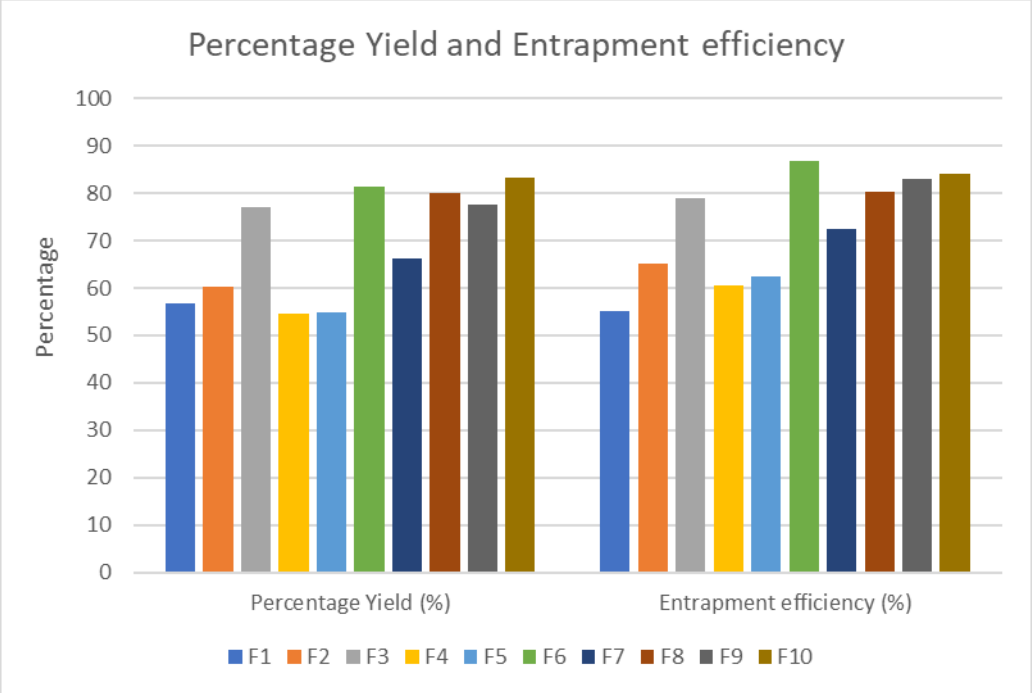

Figure 1: Column representation of percentage yield & entrapment efficiency of batch F1-F10.

In- vitro drug release study:

The in vitro drug release of formulations was studied using the dialysis tube method. The release profile of the formulation was evaluated in PBS, serving as a pseudo-physiological medium, at

pH 7.4 and 37°C. In practice, 2 ml of drug-loaded nanoparticles was placed into a dialysis tube, and the sealed tube was completely immersed in 900 ml of the release medium within a dissolution flask, with continuous stirring at 50 rpm and 37°C. Samples of 5 ml were withdrawn at various time intervals up to 2 hours, and an equal volume of fresh PBS (pH 7.4) was added to maintain the volume. The amount of drug released was quantified using a Shimadzu 1800 UV–vis Spectrophotometer at a wavelength of 296 nm under consistent analytical conditions [80].

Table 2 Percentage drug release profile of formulation batches.

Time point (hours)	**F1**	**F2**	**F3**	**F4**	**F5**	**F6**	**F7**	**F8**	**F9**	**F10**
0	0	0	0	0	0	0	0	0	0	0
1	12%	17%	16%	14%	11%	15%	13%	16%	10%	11%
2	27%	31%	33%	23%	24%	28%	22%	23%	26%	24%
3	48%	44%	51%	39%	38%	49%	46%	52%	47%	43%
4	61%	62%	66%	57%	55%	67%	61%	66%	59%	60%
5	79%	77%	82%	72%	73%	83%	78%	84%	72%	77%
6	92%	94%	96%	88%	87%	98%	90%	93%	88%	96%

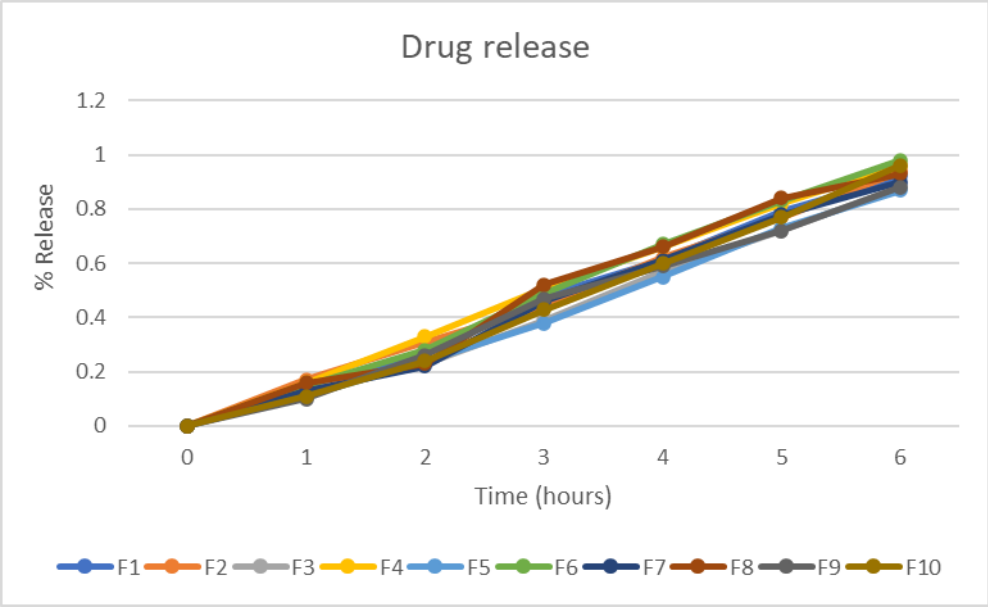

Figure 2: Cummulative drug release percentage (%).

FTIR analysis of excipients and formulation batches

FT-IR, an absorbance-based analytical technique, was utilized to characterize synthesis quality by identifying organic and polymeric compounds. In FT-IR analyses, surface-modified and drug-entrapped nanoparticle samples were examined, and the results were processed using FT-IR spectrum software [81].

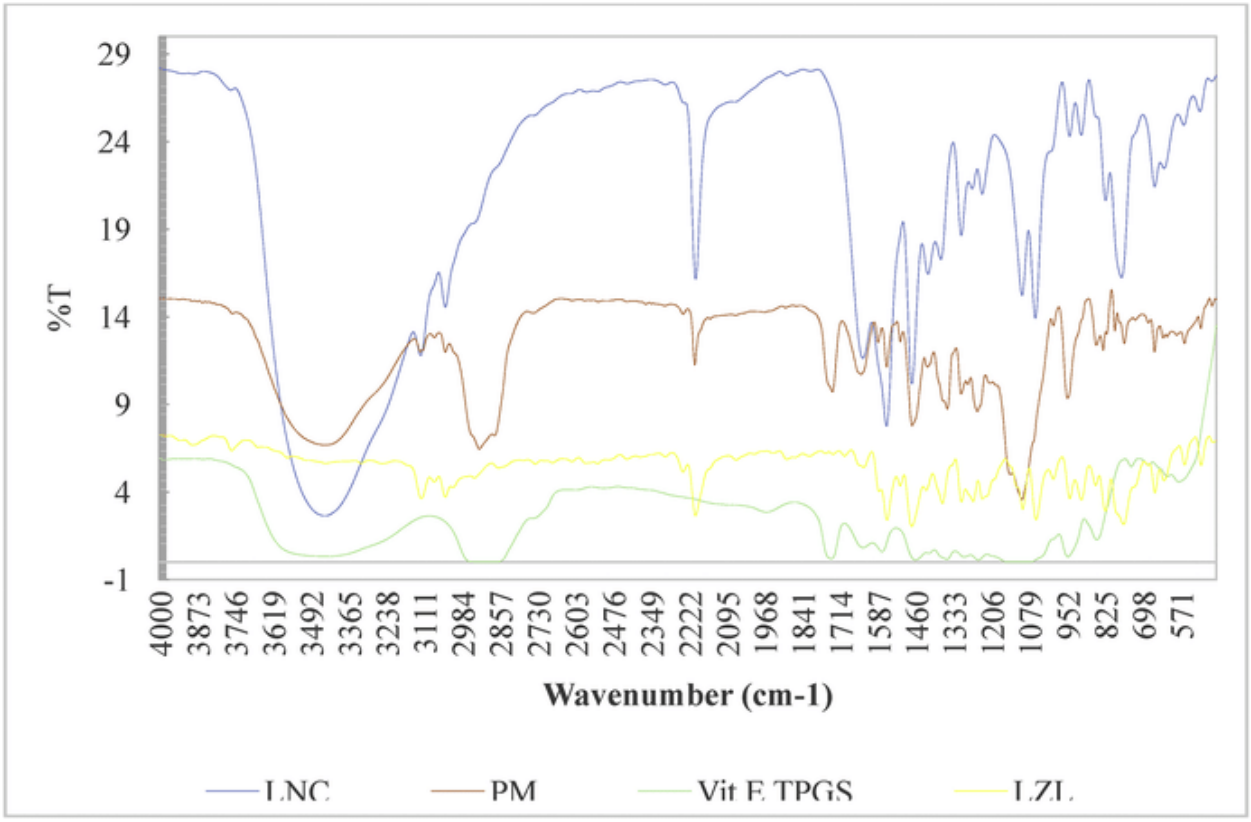

Figure 3 IR of Luliconazole

Table 3 IR interpretation of Luliconazole

Peak Range	**Group**	**Class**	**Frequencies Determined**
500–600	C─X	Bromoalkanes	501.49, 555.50
600-790	C─X	Chloroalkanes	624.94, 655.80, 763.8, 786.96
800–860	C─H	Para-disub. benzene	825.53, 856.39
900	C─H	Monosubstituted alkenes	902.69
990	C─H	Monosubstituted alkenes	995.27
~1100	C─O	Secondary alcohols	1103.28, 1643.22
1150–1200	C─O	Tertiary alcohols	1103.28, 1643.22
1220-1300	C─O	Carboxylic acids	1234.34,1265.30,1303.88,1365.60

1450-1680	C═C	AromaticC═Candconjugated C═C	1512.19,1550.77,1581.63,1627.92
1710-1810	C=O	Carboxylic Acid	1735.93,1774.51,1813.09,1859.38
1900	C=C=C	Alkene stretching bond	1890.24, 1936.53

FTIR study of excipients used.

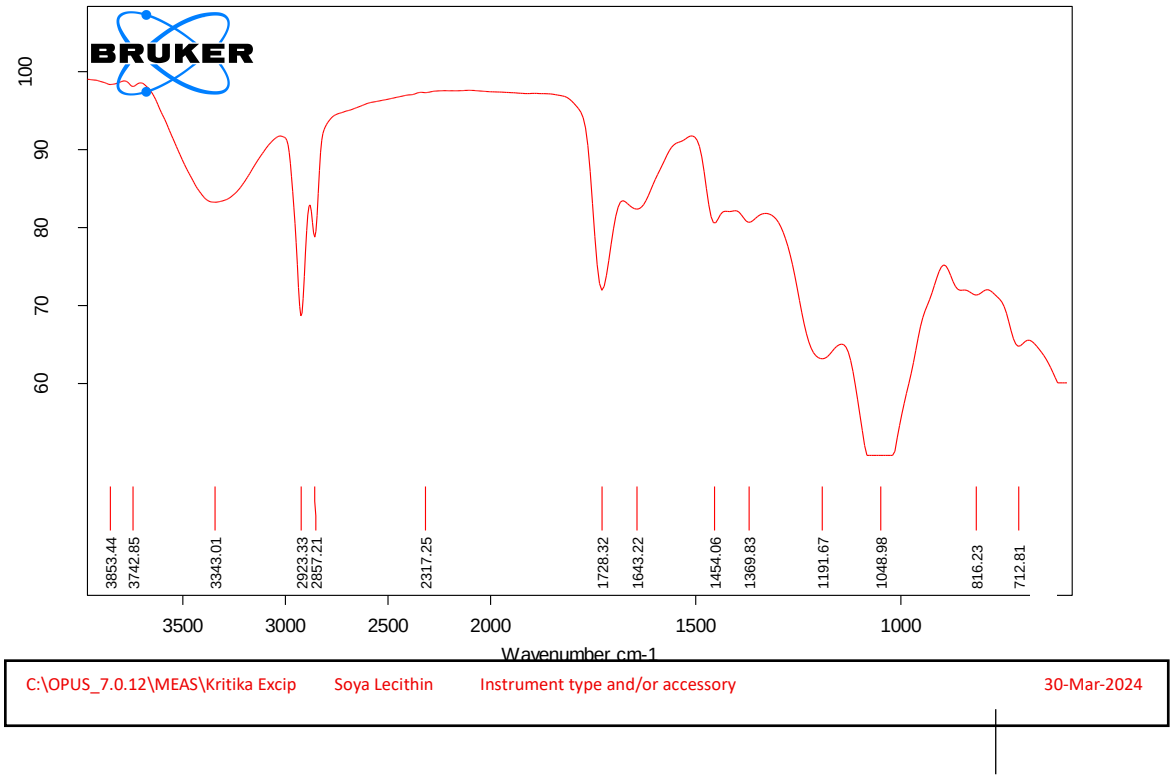

Figure 4 IR of soya lecithin

Table 4 IR interpretation of soya lecithin

Peak Range	Group	Class	Frequencies Determined
790-840	C=C bending	Alkene	816.23
1040-1050	CO-O-CO stretching	anhydride	1048.98
1163-1210	C-C stretching	Ester	1191.67
1335-1372	S=O stretching	sulfonate	1369.83
1450-1465	C-H bending	Alkane	1454.06
1640-1690	C=N stretching	imine/oxime	1643.22
1720-1740	C=O stretching	Aldehyde	1728.32
2840-3000	C-H stretching	Alkane	2857.21
2800-3000	N-H stretching	amine salt	2923.33
3310-3350	N-H stretching	secondary amine	3343.01

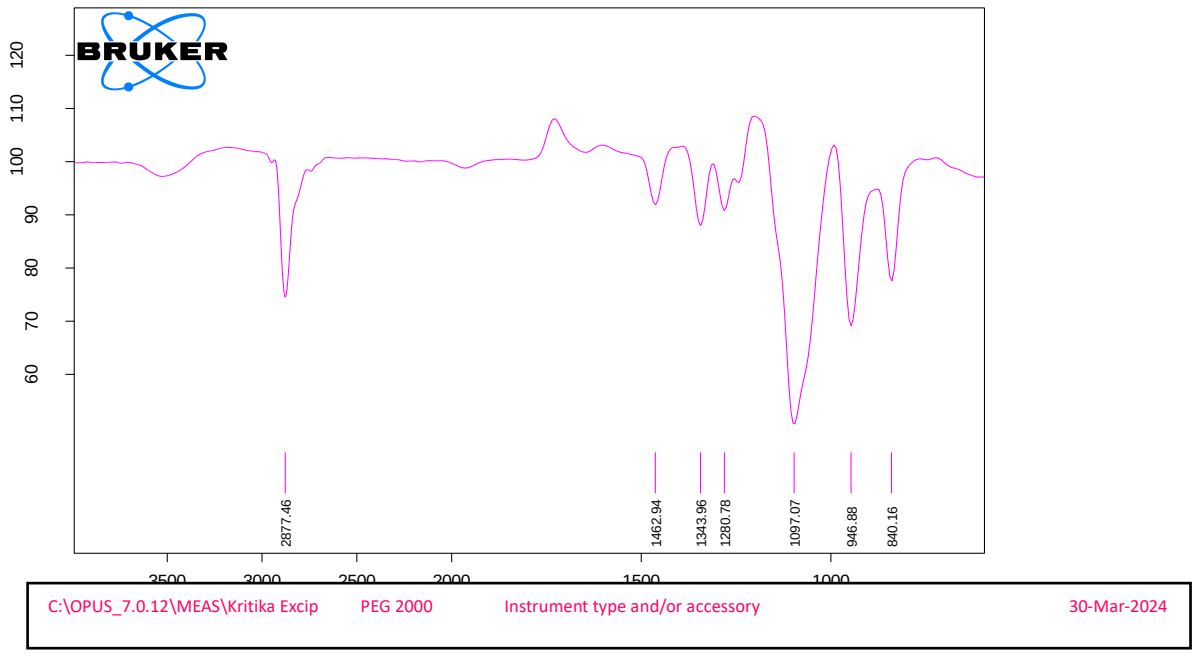

Figure 5 IR of Polyethylene glycol-2000

Table 5 IR interpretation of Polyethylene glycol-2000

Peak Range	Group	Class	Frequencies Determined
790-840	C=C bending	alkene	840.16
1085-1150	C-O stretching	aliphatic ether	1097.07
1250-1310	C-O stretching	aromatic ester	1280.78
1330-1420	O-H bending	Alcohol	1343.96
1450-1465	C-H bending	Alkane	1462.94
2840-3000	C-H stretching	Alkane	2877.46

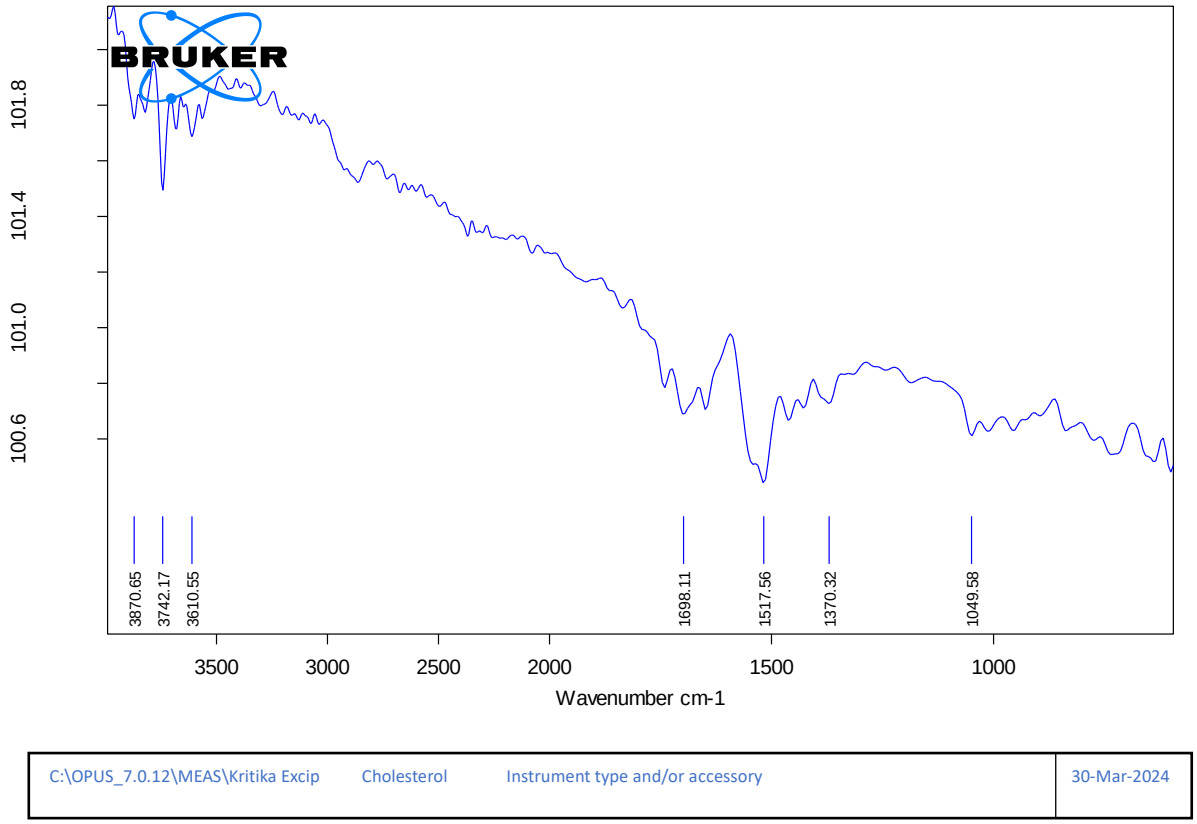

Figure 6 IR of Cholesterol-AR

Table 6 IR interpretation of Cholesterol-AR

Peak Range	Group	Class	Frequencies Determined
1030-1070	S=O stretching	Sulfoxide	1049.58
1335-1370	S=O stretching	sulfonamide	1370.32
1600-1550	N-O stretching	nitro compound	1517.56
1685-1710	C=O stretching	conjugated aldehyde	1698.11

FTIR study of Formulation batches.

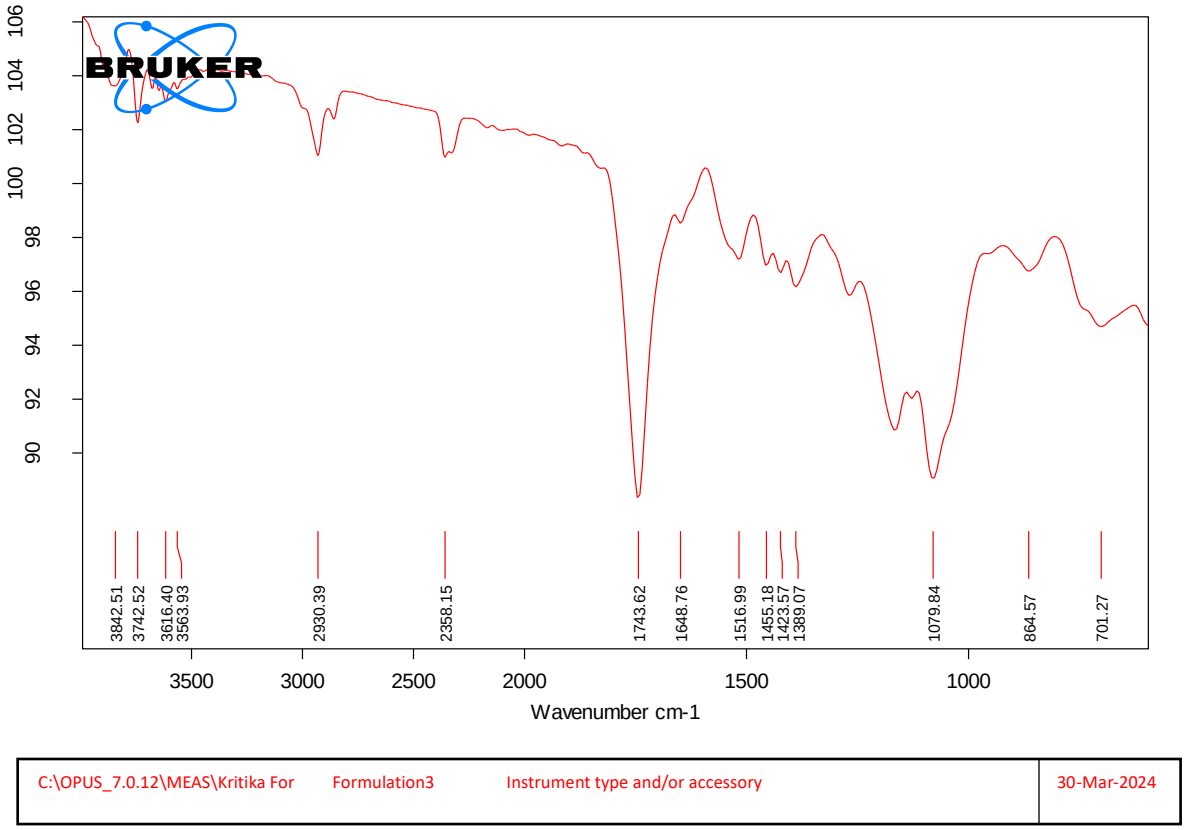

Figure 7 IR of Formulation batches F3

Table 7 IR interpretation of Formulation batch F3

Peak Range	Group	Class	Frequencies Determined
3100-3690 cm^-1	Hydroxyl O-H	Alcohols	3563.93 cm^-1
2850-2960 cm^-1	Alkane C-H	Alkanes	2930.39 cm^-1
1700-1750 cm^-1	Ketones and Aldehydes C=O	Carbonyl Compounds	1743.62 cm^-1
1350-1480 cm^-1	Alkanes CH2	Alkanes	1455.18 cm^-1
1000-1300 cm^-1	Ethers C-O	Ethers	1079.84 cm^-1
900-1000 cm^-1	Methyl groups CH3	Alkanes	970.08 cm^-1
700-800 cm^-1	Chlorinated groups C-Cl	Haloalkanes	701.27 cm^-1

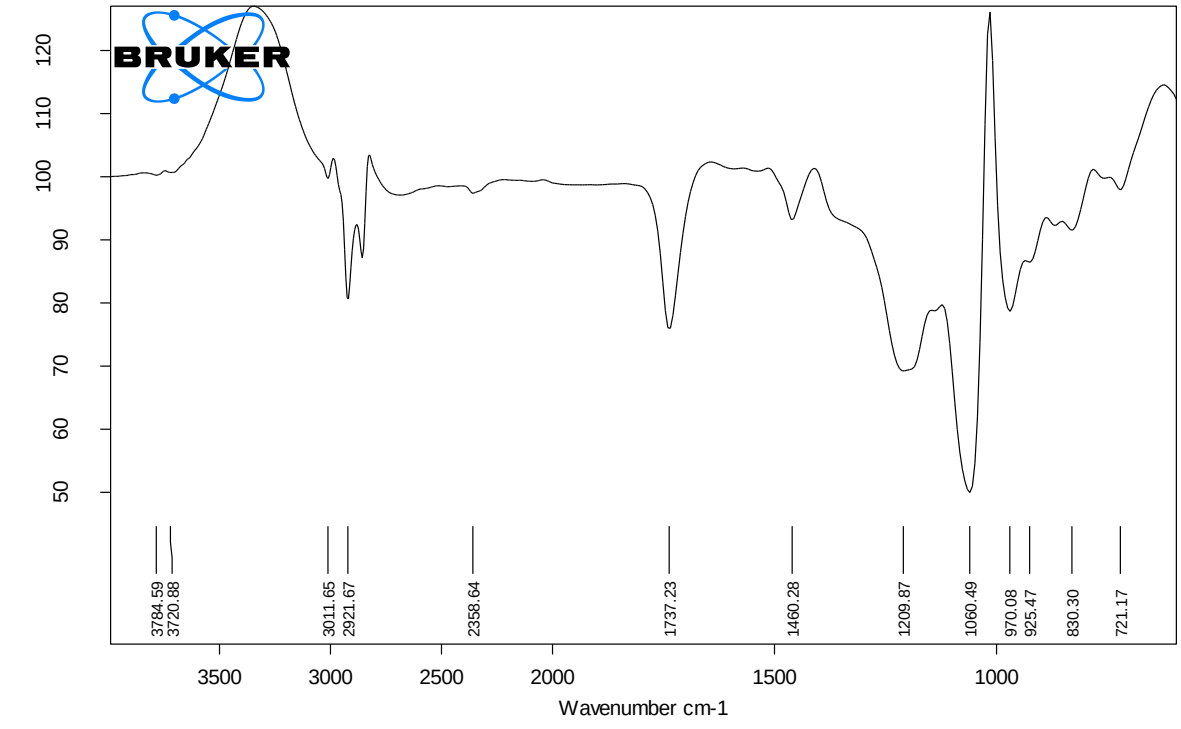

Figure 8 IR of Formulation batches F6

Table 8 IR interpretation of Formulation batch F6

Peak Range	**Group**	**Class**	**Frequencies Determined**
3000-3100 cm^-1	Aromatic compounds C-H	Aromatic hydrocarbons	3011.85 cm^-1
2850-2960 cm^-1	Alkane C-H	Alkanes	2921.67 cm^-1
1700-1750 cm^-1	Ketones and Aldehydes C=O	Ketones/Aldehydes	1737.23 cm^-1
1350-1480 cm^-1	Alkanes CH2	Alkanes	1460.28 cm^-1
1000-1300 cm^-1	Ethers C-O	Ethers	1209.87 cm^-1
900-1000 cm^-1	Methyl groups CH3	Alkyl groups	970.08 cm^-1
700-800 cm^-1	Chlorinated groups C-Cl	Halogenated hydrocarbons	721.17 cm^-1

UV- Spectrophotometric study

Wavelength determination of *Luliconazole*

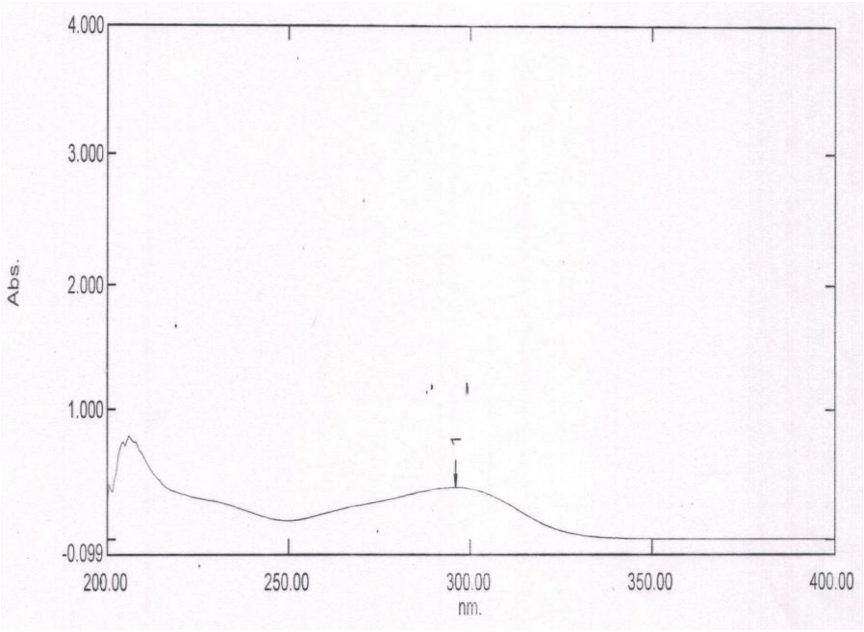

Figure .9 Lamda max determination of *Luliconazole*

Table 7.9 Wavelength determination of *Luliconazole*

No.	P/V	Wavelength	Abs.
1	↑	296.00	0.397

Figure 10 Luliconazole standard curve in DMS

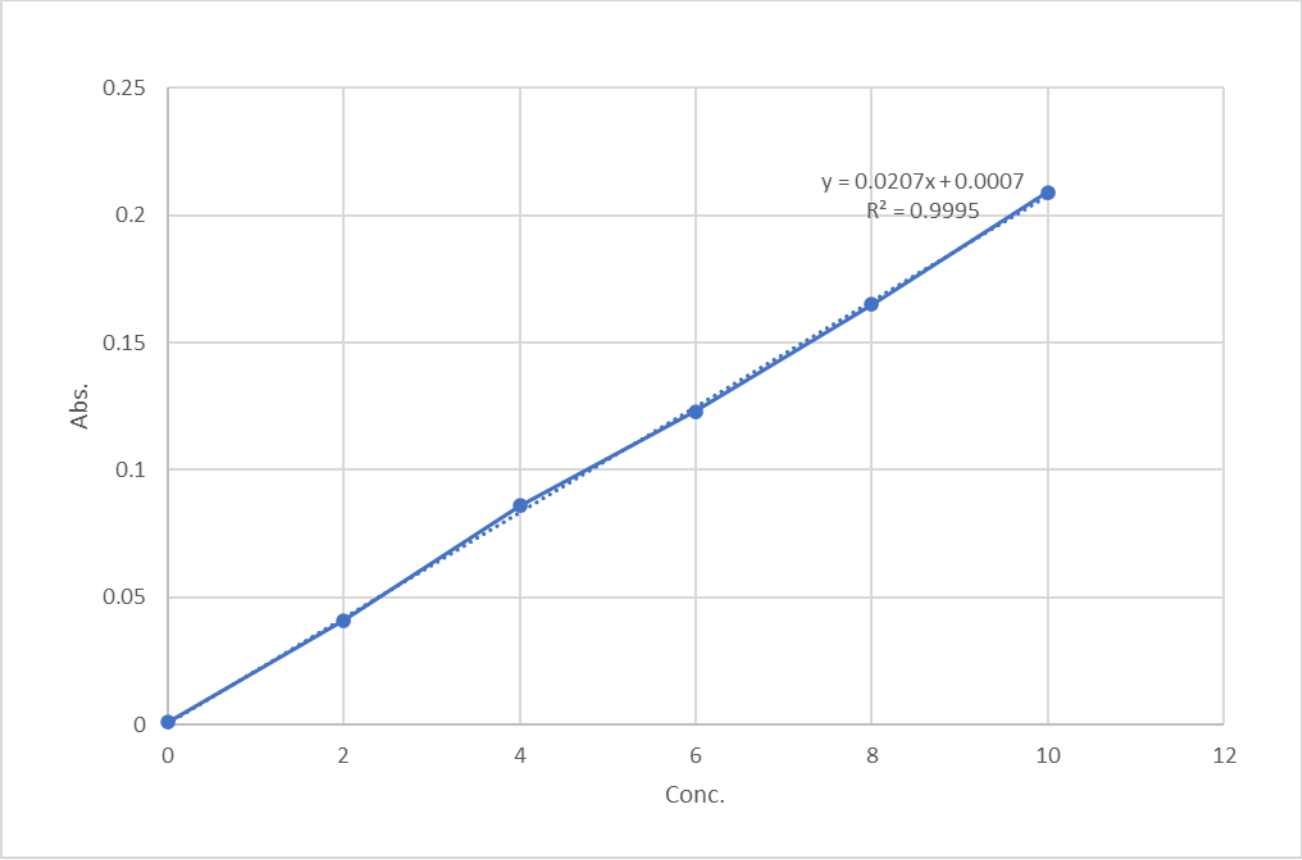

.

Table 10 Absorbance table of Luliconazole standard curve in DMSO.

Sample No.	Conc.	WL 296
1	0.000	0.001
2	2.000	0.041
3	4.000	0.086
4	6.000	0.123
5	8.000	0.165
6	10.000	0.209

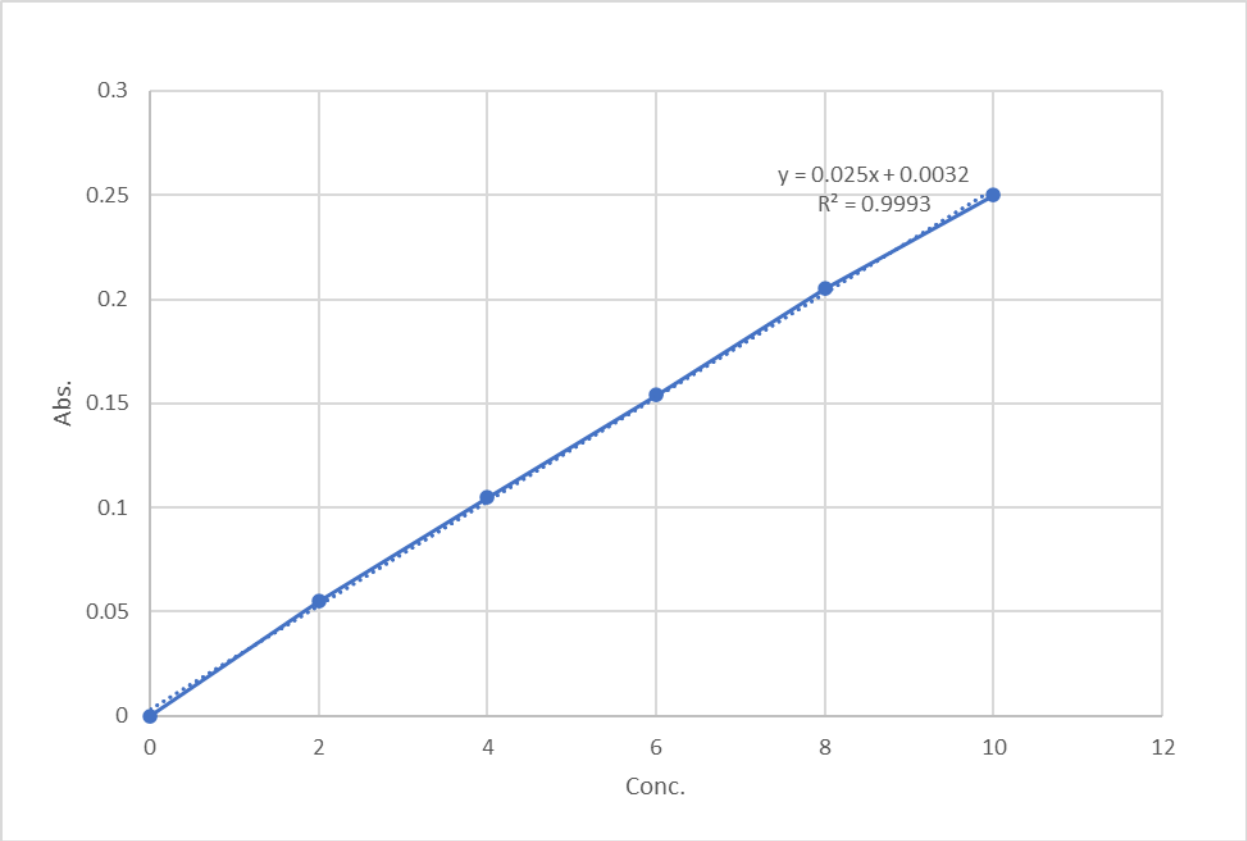

Figure 11 Luliconazole standard curve in Ethanol.

Table 11 Absorbance table of Luliconazole standard curve in ethanol.

Sample No.	**Conc.**	**WL296**
1	0.000	0.001
2	2.000	0.055
3	4.000	0.105
4	6.000	0.154
5	8.000	0.205
6	10.000	0.25

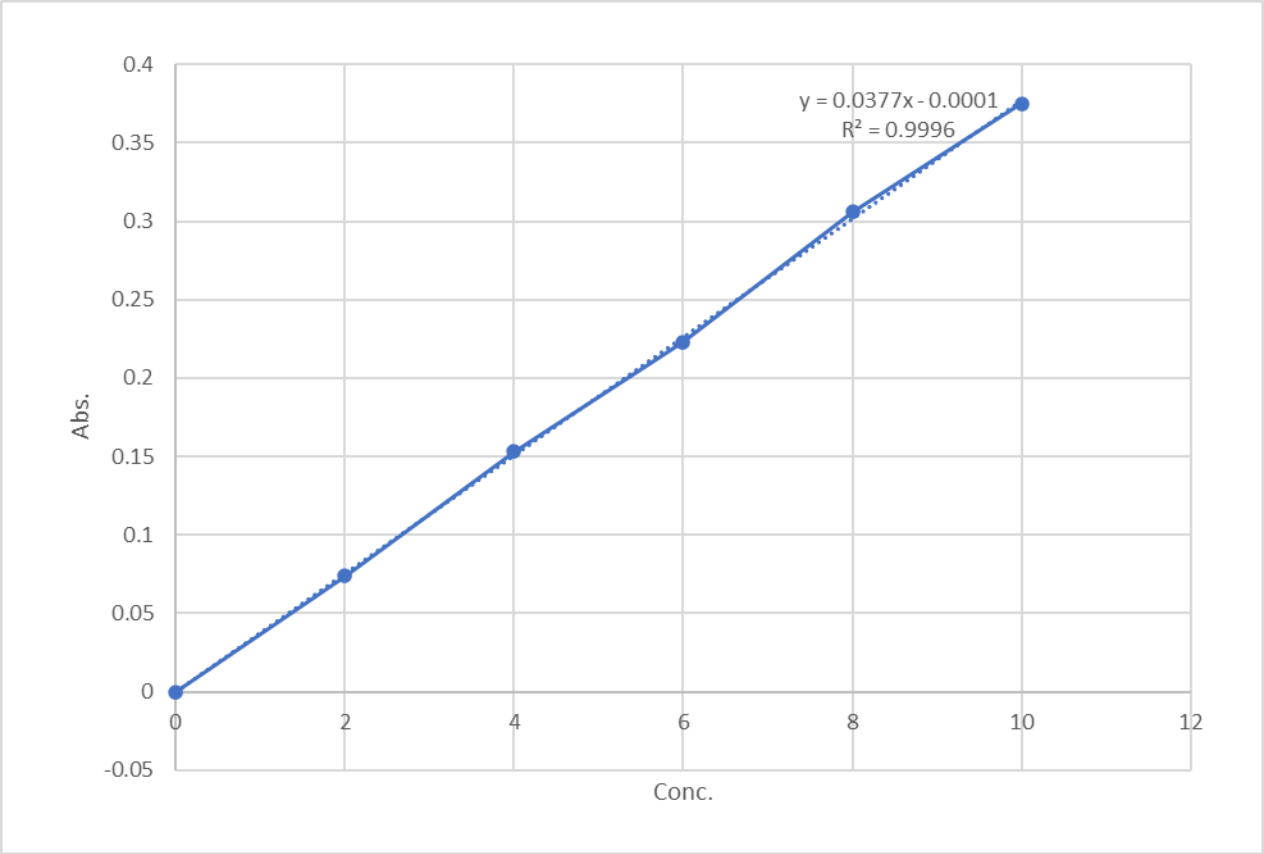

Figure 12 Luliconazole standard curve in phosphate buffer.

Table 12 Absorbance table of Luliconazole standard curve in phosphate buffer.

Sample No.	Conc.	WL296
1	0.000	0.001
2	2.000	0.074
3	4.000	0.153
4	6.000	0.223

5	8.000	0.306
6	10.000	0.375

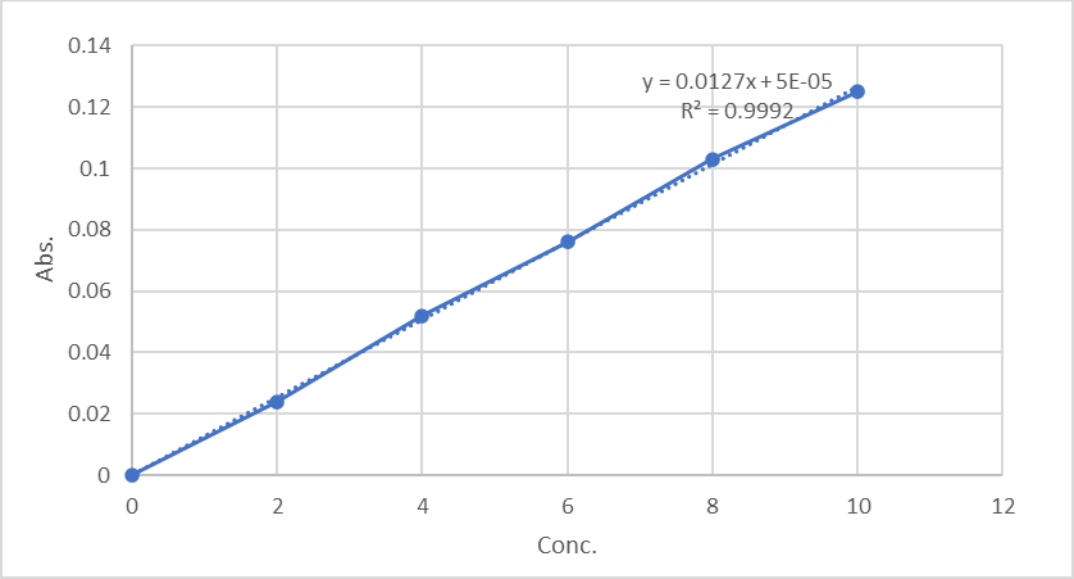

Figure13 Luliconazole standard curve in water.

Table 13 Absorbance table of Luliconazole standard curve in water.

Sample No	**Conc.**	**WL296**
1	0.000	0.001
2	2.000	0.024
3	4.000	0.052
4	6.000	0.076

5	8.000	0.103
6	10.000	0.125

Zeta-potential, particle size and Polydispersity index

Particle size and zeta potential are crucial for understanding colloidal systems. Particle size indicates the dimensions of individual particles, while zeta potential measures the electric potential at the particle surface. The table below shows particle sizes and zeta potential, with the Polydispersity Index (PDI) included to provide information on particle size distribution within each formulation. A lower PDI value indicates a more uniform particle size distribution,

while a higher value suggests a wider range of particle sizes within the formulation.

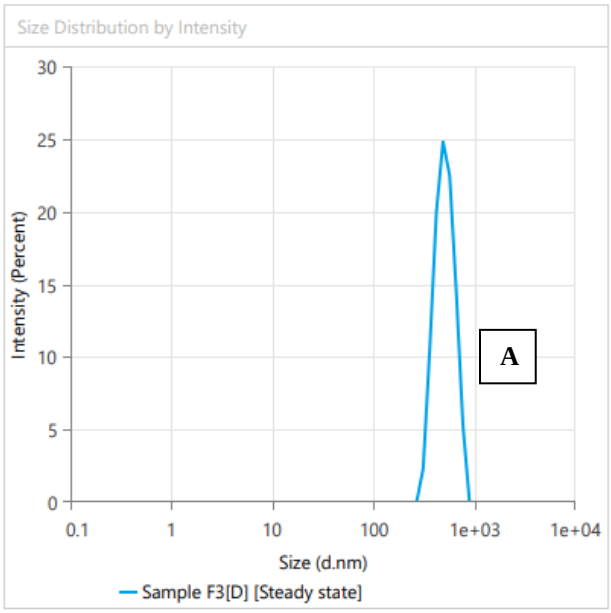

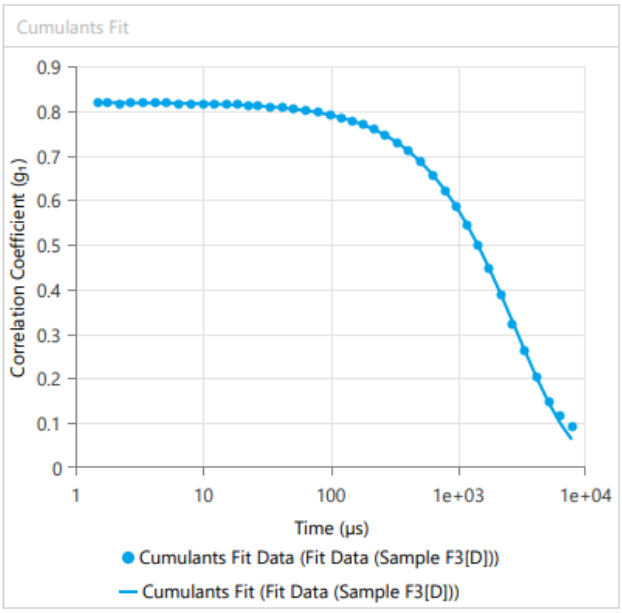

Figure 14: (A) is the size distribution graph wrt intensity and cumulant fit (B) graphical representation of batch F6

Table 14: Average size table of formulation batch F6

Name	Mean	Standard Deviation	RSD	Minimum	Maximum
Z-Average (nm)	302.2	-	-	302.2	302.2
Polydispersity Index (PI)	0.04425	-	-	0.04425	0.04425
Intercept	0.8187	-	-	0.8187	0.8187
Derived Mean Count Rate (kcps)	1569	-	-	1569	1569
Cuvette Position (mm)	4.64	-	-	4.64	4.64
Number Of Size Runs	30	-	-	30	30
Run Retention (%)	95	-	-	95	95
In Range (%)	93.61	-	-	93.61	93.61
Fit Error	0.001142	-	-	0.001142	0.001142
Detector Angle (°)	90	-	-	90	90

Table 15: Zeta potential table of formulation batch F6.

Name	Mean	Standard Deviation	RSD	Minimum	Maximum
Zeta Potential (mV)	-12.97	-	-	-12.97	-12.97
Zeta Deviation (mV)	7.327	-	-	7.327	7.327
Conductivity (mS/cm)	3.647	-	-	3.647	3.647
Quality Factor	1.729	-	-	1.729	1.729
Number Of Zeta Runs	12	-	-	12	12
Mean Count Rate (kcps)	143.3	-	-	143.3	143.3
Reference Beam Count Rate (kcps)	2479	-	-	2479	2479
Effective Voltage (V)	149.7	-	-	149.7	149.7
Measured Current (mA)	8.354	-	-	8.354	8.354
Wall Zeta Potential (mV)	-1.65	-	-	-1.65	-1.65
Attenuator	6	-	-	6	6

Table 16: Average size, zeta potential, polydispersity index of formulation batches from F1-F6

SR No.	**Batch No.**	**Z-Average (nm)**	**Polydispersity index**	**Zeta potential (mv)**
1	F4s	350.4	0.08812	-5.45

2	F9	390.8	0.09712	-10.12
3	F3	374.4	0.08974	-15.86
4	F10	335.3	0.07546	-13.89
5	F8	325.1	0.04556	-12.54
6	F6	302.2	0.04425	-12.97

Scanning Electron Microscopy (SEM)

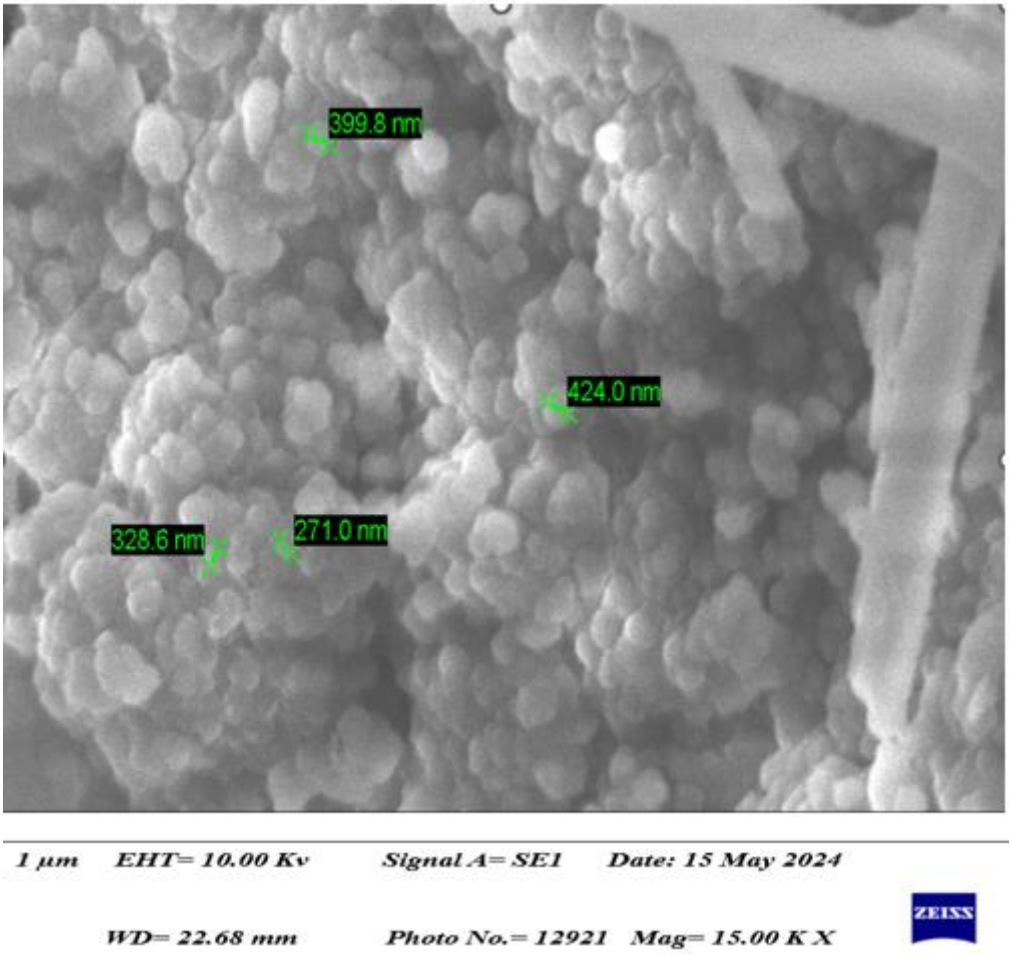
399.8 nm
424.0 nm
328.6 nm
271.0 nm
1 µm EHT= 10.00 Kv Signal A= SE1 Date: 15 May 2024
WD= 22.68 mm Photo No.= 12921 Mag= 15.00 K X
ZEISS

Conclusion

The research titled "Formulation and Evaluation of Polymeric Nanoparticles for Optimized Luliconazole Delivery in Tinea Versicolor Management" comprises seven chapters, each contributing uniquely to the overarching research theme. It serves as a foundation, highlighting the need for refined drug delivery systems to tackle the complexities of tinea versicolor management. It conducts a thorough literature review, exploring existing knowledge on tinea versicolor, luliconazole, and the potential of polymeric nanoparticles for drug delivery. This review establishes a solid framework for subsequent research. Chapter 3 outlines the research aims and objectives, providing a clear path for the following chapters. In Chapter 4, detailed profiles of luliconazole and essential excipients are presented, ensuring a comprehensive understanding of the materials used. the groundwork for nanoparticle formulation through pre-formulation studies, crucial for successful formulation. It delves into the formulation process itself, explaining the techniques and optimization strategies employed to engineer effective nanoparticles. Finally, synthesizes the findings from rigorous characterization and evaluation studies, offering insights into optimizing luliconazole delivery for tinea versicolor management. Through a range of analytical techniques such as UV, FTIR, dissolution, zeta potential, SEM, and optical microscopy analyses, this chapter provides valuable insights into the potential advancements in dermatological therapeutics. Overall, each chapter contributes significantly to understanding and advancing the field of nanoparticle-based drug delivery for tinea versicolor treatment.

References

1. Priyadharshini V. *Study on Distribution of Malassezia Species in Patients with Pityriasis Versicolor in a Tertiary Care Hospital* (Doctoral dissertation, Coimbatore Medical College, Coimbatore).
2. Zhang AY, Camp WL, Elewski BE. Advances in topical and systemic antifungals. Dermatologic clinics. 2007 Apr 1;25(2):165-83.
3. Kamaly N, Yameen B, Wu J, Farokhzad OC. Degradable controlled-release polymers and polymeric nanoparticles: mechanisms of controlling drug release. Chemical reviews. 2016 Feb 24;116(4):2602-63.

4. Waghule T, Sankar S, Rapalli VK, Gorantla S, Dubey SK, Chellappan DK, Dua K, Singhvi G. Emerging role of nanocarriers based topical delivery of anti-fungal agents in combating growing fungal infections. Dermatologic therapy. 2020 Nov;33(6):e13905.
5. Hube B, Hay R, Brasch J, Veraldi S, Schaller M. Dermatomycoses and inflammation: The adaptive balance between growth, damage, and survival. Journal de mycologie medicale. 2015 Mar 1;25(1):e44-58.
6. Zanardelli M, Skobowiat C, Kaliszuk R, Pietrzak A. Tinea Versicolor (Pityriasis Versicolor). InEuropean Handbook of Dermatological Treatments 2023 Oct 5 (pp. 1001-1008). Cham: Springer International Publishing.
7. Patterson S, Akintilo L. Tinea Versicolor and Tinea Capitis. Dermatoanthropology of Ethnic Skin and Hair. 2017:143-59.
8. Williams KA, Wondimu B, Ajayi AM, Sokumbi O. Skin of color in dermatopathology: does color matter?. Human Pathology. 2023 Oct 1;140:240-66.
9. Bonifazi E. Differential diagnosis in pediatric dermatology. Springer Science & Business Media; 2013 Oct 4.
10. Kallini JR, Riaz F, Khachemoune A. Tinea versicolor in dark-skinned individuals. International journal of dermatology. 2014 Feb;53(2):137-41.
11. Bezie Z, Deboch B, Ayele D, Workeneh D, Haile M, Mulugeta G, Belay G, Sewhunegn A, Mohammed A. Common skin diseases. Int Dev. 2005;13:200-4.
12. Rhimi W, Theelen B, Boekhout T, Aneke CI, Otranto D, Cafarchia C. Conventional therapy and new antifungal drugs against Malassezia infections. Medical Mycology. 2021 Mar;59(3):215-34.
13. Leung AK, Barankin B, Lam JM, Leong KF, Hon KL. Tinea versicolor: an updated review. Drugs in Context. 2022;11.
14. Wang L, Song X, Cheng YN, Cheng S, Chen T, Li H, Yan J, Wang X, Zhou H. 1, 2, 4-Triazole benzamide derivative TPB against Gaeumannomyces graminis var. tritici as a novel dual-target fungicide inhibiting ergosterol synthesis and adenine nucleotide transferase function. Pest Management Science. 2024 Apr;80(4):1717-27.
15. Adawiyah R, Arimurti A, Sjam R. Comparison of Selenium Sulfide 1% and Zinc Pyrithione 1% and Combination of them in Overcoming Malassezia Globosa in Vitro. eJournal Kedokteran Indonesia. 2018 May 16;6(1):237854.

16. Shen T, Huang S. Repositioning the old fungicide ciclopirox for new medical uses. Current pharmaceutical design. 2016 Aug 1;22(28):4443-50.
17. Gajubhai PH, Jain SK, Kankane M. Development and in vitro characterization of the proliposome gel of terbinafine hydrochloride. World Journal of Biology Pharmacy and Health Sciences. 2024;17(1):198-214.
18. Saha, P., Kumar, A., Bhanja, J., Shaik, R., Kawale, A. L., & Kumar, R. (2022). A review of immune blockade safety and antitumor activity of dostarlimab therapy in endometrial cancer. *International Journal for Research in Applied Sciences and Biotechnology*, *9*(3), 201-209.
19. Müller C, Staudacher V, Krauss J, Giera M, Bracher F. A convenient cellular assay for the identification of the molecular target of ergosterol biosynthesis inhibitors and quantification of their effects on total ergosterol biosynthesis. Steroids. 2013 May 1;78(5):483-93.
20. Kumar, R., Saha, P., Kumar, Y., Sahana, S., Dubey, A., & Prakash, O. (2020). A review on diabetes mellitus: type1 & Type2. *World Journal of Pharmacy and Pharmaceutical Sciences*, *9*(10), 838-850.
21. Sorgo AG, Heilmann CJ, Dekker HL, Bekker M, Brul S, de Koster CG, de Koning LJ, Klis FM. Effects of fluconazole on the secretome, the wall proteome, and wall integrity of the clinical fungus Candida albicans. Eukaryotic cell. 2011 Aug;10(8):1071-81.
22. Zhou Y, Yang H, Zhou X, Luo H, Tang F, Yang J, Alterovitz G, Cheng L, Ren B. Lovastatin synergizes with itraconazole against planktonic cells and biofilms of Candida albicans through the regulation on ergosterol biosynthesis pathway. Applied microbiology and biotechnology. 2018 Jun;102:5255-64.
23. Vishwakarma M, Haider T, Soni V. Update on fungal lipid biosynthesis inhibitors as antifungal agents. Microbiological Research. 2023 Oct 12:127517.
24. Mishra AK, Kumar A, Singh H, Verma S, Sahu JK, Mishra A. Chemistry and pharmacology of luliconazole (imidazole derivative): a novel bioactive compound to treat fungal infection-a mini review. Current Bioactive Compounds. 2019 Dec 1;15(6):602-9.
25. Baghel S, Nair VS, Pirani A, Sravani AB, Bhemisetty B, Ananthamurthy K, Aranjani JM, Lewis SA. Luliconazole-loaded nanostructured lipid carriers for topical treatment of superficial Tinea infections. Dermatologic Therapy. 2020 Nov;33(6):e13959.

26. Yang J, Liang Z, Lu P, Song F, Zhang Z, Zhou T, Li J, Zhang J. Development of a luliconazole nanoemulsion as a prospective ophthalmic delivery system for the treatment of fungal keratitis: in vitro and in vivo evaluation. Pharmaceutics. 2022 Sep 26;14(10):2052.
27. Shah MJ. *Comparative Study of Efficacy and Safety of Topical Luliconazole (1%) Versus Topical Terbinafine (1%) in Treatment of Tinea Corporis/Cruris* (Doctoral dissertation, Rajiv Gandhi University of Health Sciences (India)).
28. Amudha G. *A prospective, randomized open label study to compare the efficacy and safety of topical luliconazole 1% cream with topical terbinafine 1% cream in the treatment of tinea corporis and tinea cruris* (Doctoral dissertation, Chengalpattu Medical College, Chengalpattu).
29. Awuchi, C. G., Amagwula, I. O., Priya, P., Kumar, R., Yezdani, U., & Khan, M. G. (2020). Aflatoxins in foods and feeds: A review on health implications, detection, and control. *Bull. Environ. Pharmacol. Life Sci*, *9*, 149-155.
30. Khanna D, Bharti S. Luliconazole for the treatment of fungal infections: an evidence-based review. Core evidence. 2014 Sep 9:113-24.
31. Keshwania P, Kaur N, Chauhan J, Sharma G, Afzal O, Alfawaz Altamimi AS, Almalki WH. Superficial Dermatophytosis across the World's Populations: Potential Benefits from Nanocarrier-Based Therapies and Rising Challenges. ACS omega. 2023 Aug 22;8(35):31575-99.
32. Nami S, Aghebati-Maleki A, Aghebati-Maleki L. Current applications and prospects of nanoparticles for antifungal drug delivery. EXCLI journal. 2021;20:562.
33. Kahraman E, Güngör S, Özsoy Y. Potential enhancement and targeting strategies of polymeric and lipid-based nanocarriers in dermal drug delivery. Therapeutic delivery. 2017 Nov;8(11):967-85.